Materials Science in Semiconductor Processing 121 (2021) 105287

Contents lists available at ScienceDirect

Materials Science in Semiconductor Processing

journal homepage: http://www.elsevier.com/locate/mssp

Full length article

Bound oxygen influence on the phase composition and electrical properties of semi-insulating silicon films

Vladimir A. Terekhov [a], Dmitriy N. Nesterov [a], Konstantin A. Barkov [a], Evelina P. Domashevskaya [a,*], Aleksandr V. Konovalov [a], Yuriy L. Fomenko [a], Pavel V. Seredin [a,b], Dmitry L. Goloshchapov [a], Anatoliy I. Popov [c], Aleksey D. Barinov [c], Vyacheslav M. Andreeshchev [a], Igor E. Zanin [a], Sergey A. Ivkov [a], Oksana E. Loktionova [a]

[a] Voronezh State University, Voronezh, 394018, Russia
[b] Ural Federal University Named After First President of Russia B. N. Yeltsin, Yekaterinburg, 620002, Russia
[c] National Research University "Moscow Power Engineering Institute", Moscow, 111250, Russia

ARTICLE INFO

Keywords:
Semi-Insulating Polycrystalline Oxygen-doped Silicon
SIPOS
Silicon nanocrystals
Silicon-oxygen clusters $SiOSi_3$ type
Resistivity
Activation energy of conductivity

ABSTRACT

The purpose of this work is to establish of the bound oxygen effect on the phase composition of the Semi-Insulating Polycrystalline Oxygen-doped Silicon (SIPOS) films by means of three independent methods: X-ray diffraction (XRD), Ultrasoft X-ray Emission Spectroscopy (USXES) and Raman spectroscopy, also on their electrophysical properties, depending on the relative oxygen content in the gas mixture flow ($\gamma=N_2O/SiH_4$) of the plasma reactor during the chemical vapor deposition of submicron SIPOS layers on monocrystalline silicon wafers.

The increase in the oxygen content in SIPOS layers from $\gamma=0$ to maximum at $\gamma=0.15$ leads to the reduction of Si nanocrystals size from ~75 nm to 2–5 nm, submerged in amorphous matrix.

Oxygen is contained in the bound form of silicon-oxygen clusters $SiOSi_3$ type in the amorphous silicon matrix without SiO_2 formation.

These nonlinear qualitative and quantitative changes in the atomic structure of the SIPOS layers under the influence of bound oxygen increase not only the resistivity of the films by two orders of magnitude but also the activation energy of conductivity in comparison with silicon at the temperatures above room temperature.

1. Introduction

Semi-Insulating Polycrystalline Oxygen-doped Silicon (SIPOS) films allow one to significantly increase the breakdown voltage of discrete high-voltage devices [1,2] by reducing the effect of charge accumulation caused by injection of the hot current carriers into dielectric layer. The resistivity of these films strongly depends on the oxygen content and increases from $2\cdot10^6$ Ohm·cm (in the films without oxygen) to $\sim10^{10}$ Ohm·cm (with the oxygen content of about 30 at.%) [3–8]. At the same time, the changes in the activation energy of conductivity are also observed [3–8]. In the works of different authors its values vary considerably under close oxygen concentrations. As our later research showed [9], the adding of oxygen during the growth of SIPOS films leads to the appearance of amorphous silicon phase (*a*-Si) and amorphous non-stoichiometric silicon oxide phase (*a*-SiO_x, where *x* can vary from 0.5 to 2) in their composition. As the oxygen concentration increases, so does the content of amorphous *a*-Si and *a*-SiO_x phases. With the oxygen content in the SIPOS film is about 15 at.%, it consists mainly of the amorphous phases, the presence of which is difficult to analyze by means of diffraction methods. That leads to the existence of significantly different models of the structure of SIPOS composite films [4–7].

The purpose of this work is to determine the effect of bound oxygen on the phase composition of SIPOS films by means of three independent methods as well as on their electrophysical properties, depending on the relative oxygen content in the gas mixture within the interval for $\gamma=N_2O/SiH_4=0\div0.15$ in plasma reactor during gas-phase deposition of submicron SIPOS layers on single-crystal silicon wafers.

* Corresponding author.
E-mail address: ftt@phys.vsu.ru (E.P. Domashevskaya).

https://doi.org/10.1016/j.mssp.2020.105287
Received 31 January 2020; Received in revised form 28 May 2020; Accepted 27 June 2020
Available online 5 August 2020
1369-8001/

2. Experiment

SIPOS films were obtained by means of the standard technique of low pressure chemical vapor deposition (LP CVD) of SiH_4 silane (SiH_4 flow rate 8 l/h) with the addition of N_2O as an oxygen source at P=20 Pa and temperature of 625 °C. The proportion of nitrous oxide in gas mixture SiH_4+N_2O varied within $\gamma=N_2O/SiH_4=0$ 0.15. The thickness of SIPOS films was of 300 nm. The films were deposited on the oxidized Si(100) and Si(111) substrates with thermal oxide SiO_2 film thickness of ~100 nm. To perform electrical measurements, the groups of aluminum contacts of various sizes were deposited on SIPOS films.

The SIPOS films resistance and resistivity were calculated from the Current-Voltage characteristics. Measurements of Current-Voltage (I–V) characteristics were realized in the planar geometry of a sample and to the couple of aluminum contacts DC voltage were applied. Since the external load was rather large, the source worked in the voltage generator mode and the output voltage was monitored by digital voltmeter. The magnitude of the current in the circuit across the source and the film was measured with a KEITLEY-427 picoampermeter.

A study of the phase composition of SIPOS films was performed by means of three independent methods:

(1) X-ray diffraction method with a PANalytical Empyrean B.V. diffractometer employing monochromatic Cu $K_{\alpha1}$radiation and using the ICDD PDF-2 database [10];
(2) Ultrasoft X-ray Emission Spectroscopy (USXES) by recording the emission Si $L_{2,3}$ spectra, representing the density of states distribution in the valence band of silicon. Simulation of the experimental Si $L_{2,3}$ spectra using reference spectra makes it possible to determine the contribution of amorphous, crystalline, and oxide/suboxide silicon phases [9].
(3) Raman spectroscopy was also effectively used to analyze the ratio between nanocrystalline and amorphous silicon phases with a variable oxygen content in the films [11]. Raman spectra were obtained with Raman Microscope RamMics M532 EnSpectr in the range of 350–3650 cm^{-1} using laser with the wavelength of 532 nm and radiation power of 30 mW.

3. Results

3.1. X-ray diffraction investigations

Fig. 1 shows the diffraction patterns of SIPOS films obtained at the different values of technological parameter in the interval for γ=0÷0.15, affecting oxygen content in the deposited layer. In the same figure the diffraction pattern of polycrystalline silicon powder (Poly-Si) is shown as a reference. The results presented in Fig. 1 show that in SIPOS layer obtained at technological parameter value γ=0 (in the absence of nitrous oxide in the gas mixture) the Si(111), Si(220) and Si(311) reflections are observed, but their intensity decreases rapidly with the growth of γ. As it is shown in XRD patterns (Fig. 1-a), the reflections of silicon in SIPOS (γ=0) film are broadened in comparison with polycrystalline silicon powder. Next the reflection peaks of Si(220) from all of the films with different values γ were obtained with a higher exposure (Fig. 1-b). Fig. 1-b shows that an increase of γ (i.e. an increase of the oxygen content in the SIPOS films) leads to a decrease of the intensity in the Si(220) reflection and an increase in its width. Reducing in the intensity of silicon reflections indicates a decrease in the content of the crystalline phase of silicon in the film. The apparent increase in the width of the reflexes may be due to a decrease in the average size of the crystallites. Also Fig. 1-b shows the results of approximation (solid lines) of the experimental curves (points) of reflections Si(220) by Gaussians (dashed lines), and that made it possible to determine the widths of the reflections and estimate the average Si crystals size D using the Debye-Scherrer formula:

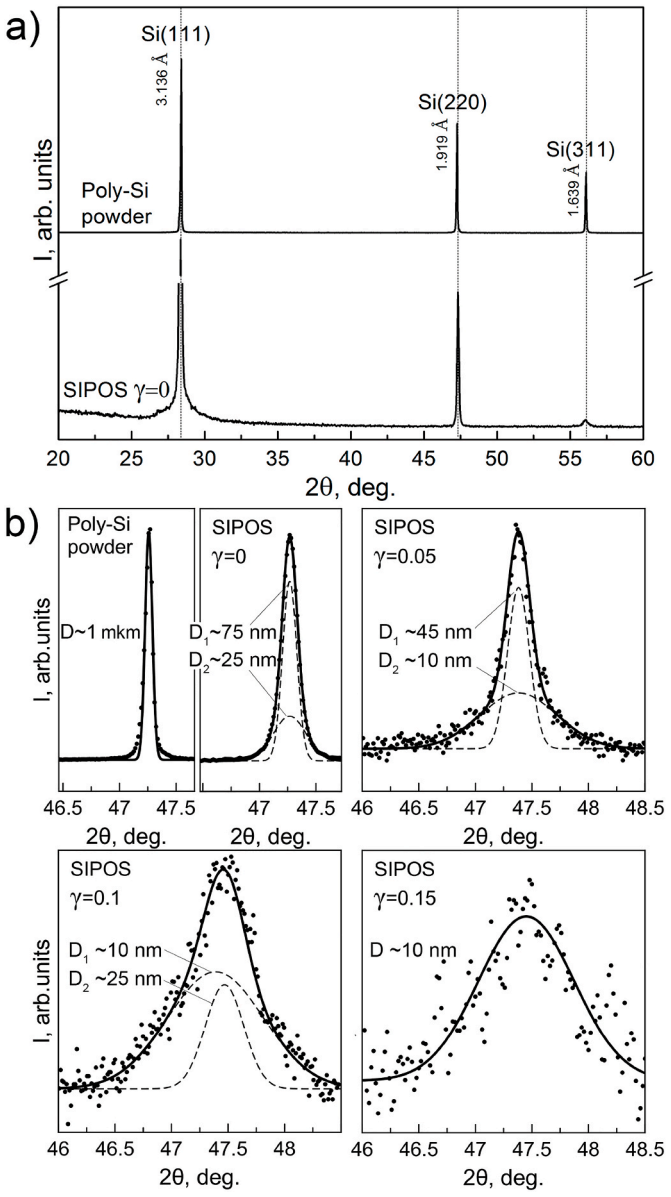

Fig. 1. (a) Diffraction patterns of SIPOS films with different oxygen content and polycrystalline silicon powder; (b) Diffraction patterns of the Si(220) reflection peak, recorded with higher exposure (dots) and results of their approximation (solid lines) by Gaussians (dashed lines).

$$D=\frac{\lambda}{\beta\cos\theta},$$

where $\beta=\sqrt{B^2-b^2}$, B is the half-width of the reflection curve of the sample, b is the half-width of the reference curve of the Poly-Si powder, λ is the wavelength of Cu $K_{\alpha1}$ radiation (1.5406 Å) and θ is the diffraction angle for the Si(220) reflection.

It should be noted that the optimal approximation of the experimental reflection curves (γ=0÷0.1) is obtained using two Gaussians and only one Gaussian is enough at γ=0.15 due to the high noise level. As a result, for three samples (γ=0; 0.05 and 0.1) two different values of nanocrystal sizes were obtained as can be seen in the diffraction pattern (Fig. 1-b). Based on the above XRD data, as the oxygen content in the film increases from γ=0 to γ=0.15, the size of nanocrystals decreases from ~75 nm to ~10 nm.

3.2. Ultrasoft X-ray emission Si $L_{2,3}$ spectra of SIPOS films

Ultrasoft X-ray emission Si $L_{2,3}$ spectra are very sensitive to the local environment of atoms, the lengths and angles of the chemical bond [9]. X-ray emission Si $L_{2,3}$ band of crystalline silicon *c*-Si (top curve in Fig. 2) has two characteristic maxima at 89.5 and 92 eV, corresponding to the density of states distribution in two low-energy silicon valence sub-bands: *s*-symmetry (first sub-band) and *s,p*- (second sub-band). The high-energy part of crystalline silicon valence band is formed by contribution of *s*-states to the two top valence *p*-sub-bands (third and fourth). In the Si $L_{2,3}$ spectrum of amorphous silicon (Fig. 2) large changes are observed, resulting from disorder in the lengths and bond angles, disturbances in the coordination number. These changes are showed in a smearing of the density of states in the valence band of *a*-Si and smoothing all features of the fine structure as compared to the spectrum of crystalline silicon *c*-Si (Fig. 2). During formation of silicon-oxygen chemical bonds a gradual shift of the main maximum of Si $L_{2,3}$ spectra from the energy value of 89.5 eV (for $SiO_{0.47}$ suboxide) to 94.5 eV (for SiO_2) is observed where O *2p*-binding orbital of oxygen is located [9]. Moreover, a part of silicon *s*-states density is just in the energy range of O *2s*-orbitals of oxygen and manifests itself in the form of long-wave satellite at 76–77 eV.

Thus, a high sensitivity of the USXES to the type of surrounding atoms, as well as to disorder in the position of atoms proved to be very important instrument for analysis of SIPOS films.

The role of oxygen in the amorphization of SIPOS films structure can be clearly seen in Si $L_{2,3}$ spectra on Fig. 2. Si $L_{2,3}$ spectrum of a SIPOS film (γ=0) with average-sized silicon nanocrystals of about 75 nm has two main maxima in the density of valence states at E ~92 eV and E~89.6 eV with a minimum between them (E~90.7 eV). As the oxygen content in SIPOS films (γ=0.05 and 0.1) increases, the minimum at 90.7 eV is hardly observed while at the highest value γ=0.15 the Si $L_{2,3}$ spectrum of SIPOS film becomes similar to that of amorphous silicon *a*-Si (Fig. 2).

In addition, a more precise analysis of the Si $L_{2,3}$ spectra of SIPOS films shows that as the oxygen content in SIPOS films increases, the intensity of the spectrum in the region of *E*~94.5 eV rises from 0.5 arb. units at γ=0 to 0.62 arb. units at γ=0.15. According to Refs. [12], the Si *3s,p*+O *2p* binding orbital is at this energy region. For this reason a rising of the number of Si–O bonds with an increase of oxygen content in the SIPOS films leads to an increase of the Si $L_{2,3}$ spectrum intensity at the energy $E \sim 94.5$ eV.

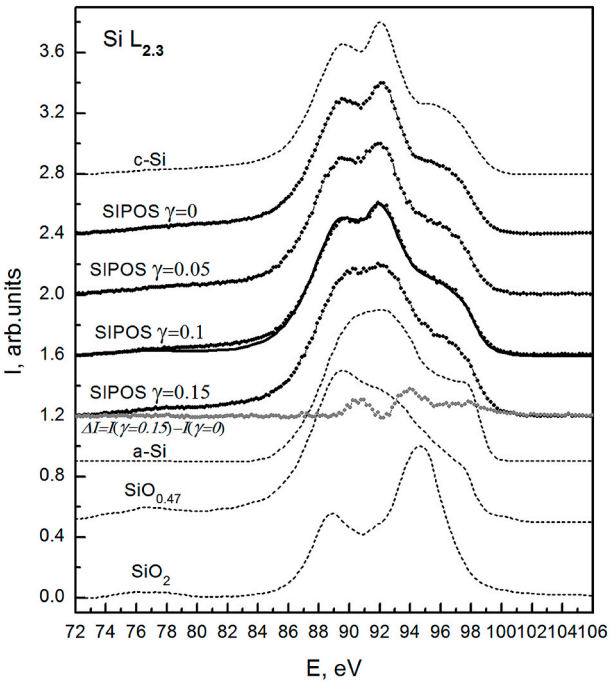

Fig. 2. Ultrasoft X-ray emission Si $L_{2,3}$ spectra of SIPOS films obtained at different values of γ (points), simulated spectrum (solid line), difference spectrum $\Delta I=I(\gamma=0.15)-I(\gamma=0)$ (gray dots) and reference spectra of crystalline silicon *c*-Si, amorphous silicon *a*-Si, silicon suboxide $SiO_{0.47}$, and silicon dioxide SiO_2 (dashed lines).

This increase in the intensity is clearly observed in the difference spectra of SIPOS films with γ=0.15 and γ=0 $\Delta I=I(\gamma=0.15)-I(\gamma=0)$, shown in Fig. 2. In the difference spectra two maxima in the middle part of the valence band at *hv*~94.0 eV and *hv*~90.7 eV are observed. The first of the maxima is caused by the appearance of Si–O bonds and the second maxima – by amorphization of the SIPOS film at γ=0.15.

The mathematical simulation of the spectra shown in Fig. 2 using reference Si $L_{2,3}$ spectra of *c*-Si, *a*-Si, $SiO_{0.47}$ and SiO_2 allowed us to estimate the content of these phases in SIPOS films (Table 1). The simulated spectrum (solid line) as an example for a SIPOS film (γ=0.1) is shown in Fig. 2. A good agreement between the experimental (points) and simulated (solid line) spectra indicates the reliability of the simulation results given in Table 1.

As it can be seen from Table 1, the SIPOS film (γ=0) obtained without addition of nitrous oxide, contains ~15 % of amorphous silicon phase concentrated on disordered boundaries of nanocrystals with an average size of ~75 nm. The introduction of oxygen into the film leads to the appearance in the SIPOS sample (γ=0.05) of a silicon suboxide phase $SiO_{0.47}$. The Si $L_{2,3}$ spectrum of this suboxide phase was first obtained in Ref. [12]. As the γ value increases, so does the content of this suboxide phase $SiO_{0.47}$ in the samples (Table 1) without the formation of silicon dioxide SiO_2. The absence of SiO_2 dioxide in SIPOS films, even with a sufficiently high oxygen content (~44 at.%) was revealed by means of XPS method in the papers [4,13].

Thus, based on the results of USXES, we propose to consider SIPOS as an amorphous -crystalline silicon matrix in which oxygen forms $SiOSi_3$ clusters corresponding to the known phase of the $SiO_{0.47}$ suboxide. The USXES data show that in SIPOS films oxygen forms of $SiOSi_3$ type clusters with silicon, where the silicon atom is surrounded by three silicon atoms and one oxygen atom.

Fig. 3 illustrates the dependence of $SiOSi_3$ type clusters ($SiO_{0.47}$ suboxide phase) content in SIPOS films as a function of the technological parameter γ value.

3.3. Raman spectroscopy

Raman spectroscopy is effectively used not only to analyze the ratio between nanocrystalline and amorphous silicon phases in the SIPOS films with different oxygen content, but also to estimate the size of silicon nanocrystals by transverse mode vibrations (TO) in the Raman spectra [11,14–16].

Fig. 4 shows experimental Raman spectra (dots) (the wavelength of exciting radiation λ=532 nm) in SIPOS films with different values of γ, together with the results of their decomposition by Gauss functions (dashed lines) into components corresponding to the crystalline, nanocrystalline and amorphous phases of silicon. The simulation results of the Raman spectra are presented as solid lines on the experimental spectra. The upper Raman spectrum belongs to a single-crystal Si substrate on which SIPOS films were deposited, and the lower Raman spectra of *a*-Si and *c*-Si [14] are given as reference spectra for comparison.

Table 1
Phase composition of SIPOS films by the data of Si $L_{2,3}$ spectra simulation.

Sample name	*nc*-Si, %	*a*-Si, %	$SiO_{0.47}$, % ($SiOSi_3$ clusters)	Error, %
SIPOS $\gamma = 0$	85	15	–	5
SIPOS $\gamma = 0.05$	30	50	20	
SIPOS $\gamma = 0.10$	20	50	30	
SIPOS $\gamma = 0.15$	–	65	35	

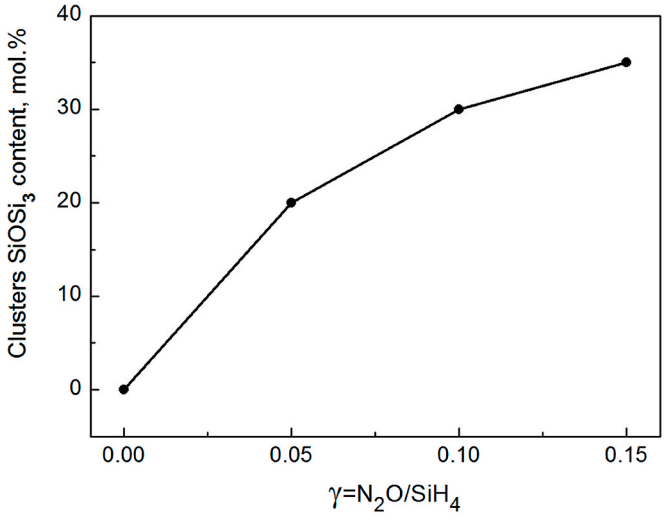

Fig. 3. The dependence of the content of $SiOSi_3$ type clusters in SIPOS films as a function of the value of technological parameter γ.

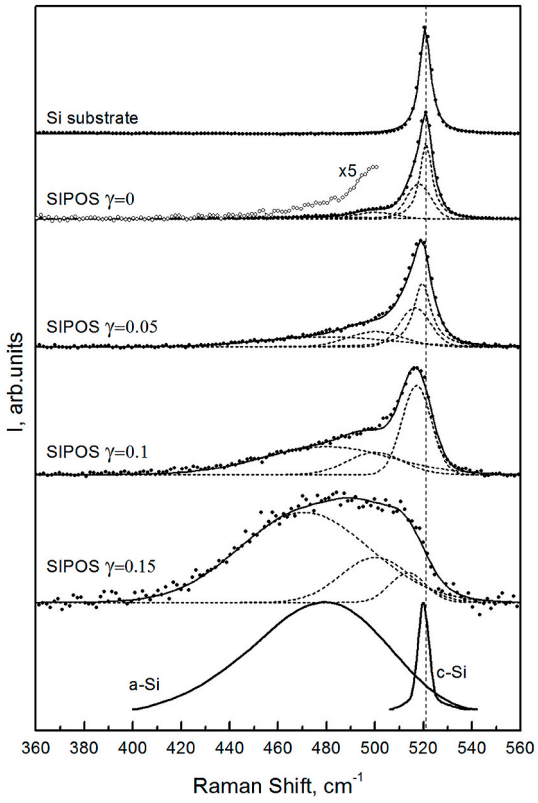

Fig. 4. Raman spectra (excitation laser wavelength λ=532 nm) in SIPOS films with different γ values (points) and the result of their decomposition (solid lines) into crystalline, nanocrystalline and amorphous components by Gaussian functions (dashed lines). The Raman spectra of *a*-Si and *c*-Si [14] are presented in the lower part of the figure.

Raman spectroscopic data (Fig. 4) also indicate a gradual amorphization of films with an increase in γ values. Raman scattering reveals that even at γ=0, i.e. in the film of nanocrystalline silicon non-doped with oxygen, the spectrum is broadened in comparison with single-crystal silicon and an additional maximum appears at $\Delta\nu\sim500$ cm^{-1}. Modeling and analysis of the Raman spectrum reveals the presence of nanocrystals with sizes ≥15 nm in the film, as evidenced by the most intense narrow peak at $\Delta\nu=521$ cm^{-1} [1,3,4,14–16], which does not contradict the of XRD data on the presence of nanocrystals in this sample with an average size of about 75 nm. In addition, the presence of a broad peak of low intensity at $\Delta\nu\approx518$ cm^{-1} and especially at $\Delta\nu\approx500$ cm^{-1} – indicates the presence of smaller nanocrystals with the size of 5–8 nm and 2–4 nm in this film, respectively [11,14–16]. In the Raman spectrum of this sample, the presence of a small amount of the amorphous phase is also possible, which can be observed as a shoulder at $\Delta\nu\sim480$ cm^{-1} [11, 14–16]. However, the content *a*-Si in this sample is not more than 10% (Table 2), that is consistent with the USXES data.

The adding of a small amount of oxygen (γ=0.05) leads to noticeable changes in the Raman spectrum (Fig. 4). The main maximum shifts and decomposes into two components located at 520 cm^{-1} and 517 cm^{-1}, corresponding to nanocrystals with average sizes D~10–15 nm and even smaller size D~5–6 nm, respectively. A significant increase of the peaks intensity at $\Delta\nu\sim500$ cm^{-1} and 480 cm^{-1} (Fig. 4) indicates at the increase in the relative contribution of nanocrystals ~2–4 nm ($\Delta\nu\sim500$ cm^{-1}) and a noticeable contribution of the amorphous phase up to about 25% ($\Delta\nu\sim480$ cm^{-1}).

When the oxygen content in the film increases to γ=0.1, the contribution of large crystals disappears in the Raman spectrum, which leads to a shift of the main maximum to 517 cm^{-1} and an increase in intensity at $\Delta\nu\sim500$ cm^{-1}. Small nanocrystals appear at $\Delta\nu\sim517$ cm^{-1} (D~5 nm) and $\Delta\nu\sim500$ cm^{-1} (D~2–4 nm) and the contribution of amorphous silicon increases up to ~50%.

With an increase to γ=0.15 the contribution from the amorphous phase (~75%) and from nanocrystals with average size ~2–4 nm predominates in the Raman spectrum (Fig. 4).

Thus, the doping of polysilicon with oxygen leads to a gradual decrease of the small crystals size from several tens to several units of nanometers and a parallel increase in the content of the amorphous silicon phase. With a relatively low level of oxygen doping at γ≤0.15, the oxygen atoms are embedded into amorphous silicon network in the form of $SiOSi_3$ clusters and the amount of bound oxygen determines the number of these clusters corresponding to the known phase of the $SiO_{0.47}$ suboxide.

3.4. *Electrical properties of SIPOS films*

Let us consider how the changes in the phase composition and structure of semi-insulating silicon affect its electrical properties. As can be seen from Fig. 5-a, when the voltage changes from 0 V to 5 V, the I–V characteristics of SIPOS films are linear, which makes it easy to calculate the resistivity. Fig. 5-b shows the dependence of the resistivity SIPOS films on the technological parameter γ. As can be seen from Fig. 5-b, the change of N_2O content in the gas mixture within the range of γ=0÷0.15 allows to increase the resistivity of the SIPOS films by approximately two orders of magnitude. To estimate the conduction activation energy, we measured the resistance of the films as a function of temperature in the range of 295–500 K.

Fig. 6 shows the dependences of the SIPOS films conductivity,

Table 2
The ratio of crystalline and amorphous silicon phases in SIPOS films by Raman spectroscopy data.

Sample name	*nc*-Si, %	*a*-Si, %	Si nanocrystals average size, nm
SIPOS γ = 0	90	10	2–4 5–6 >15
SIPOS γ = 0.05	75	25	2–4 5–6 >15
SIPOS γ = 0.1	50	50	2–4 5–6
SIPOS γ = 0.15	25	75	2–4 5–6

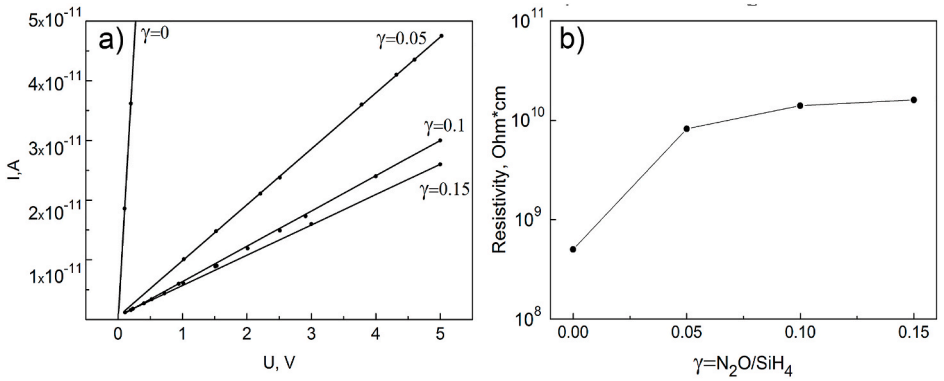

Fig. 5. (a) I–V characteristics of SIPOS films obtained with different values of γ; (b) Resistivity of SIPOS films depending on the value of the technological parameter γ.

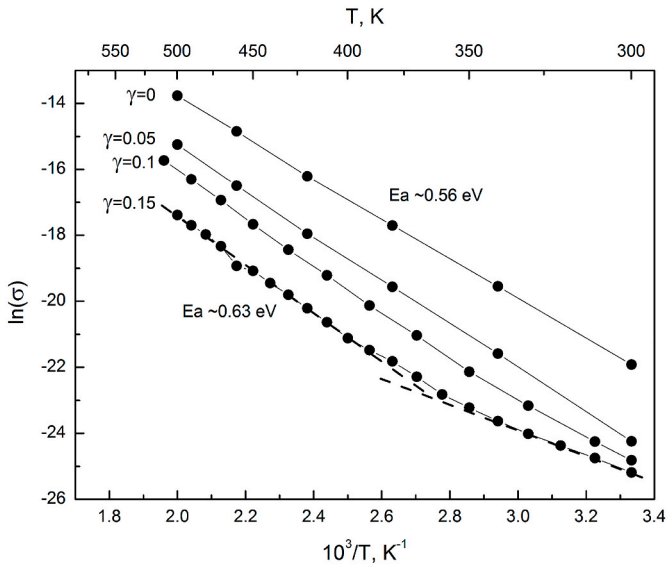

Fig. 6. Electrical conductivity of SIPOS films with different values of the technological parameter γ vs reciprocal temperature.

obtained for different values of γ within the indicated temperature range. Based on the above presented dependences, it is seen that the incorporation of oxygen into the film does not only lead to an increase in its resistance, but also to that in the activation energy of conductivity.

For a SIPOS film obtained without adding nitrous oxide the linear dependence lnσ(1/T) has a slope, which determines the activation energy of conductivity equal to 0.56–0.55 eV, corresponding to silicon. The appearance of oxygen in the SIPOS film at γ=0.05 causes an increase in resistance (Fig. 6), but has little effect on the magnitude of the activation energy. However, a further increase in the content of bound oxygen in SIPOS layers obtained at γ=0.1 leads to a slight decrease in the slope angle in the temperature dependence lnσ(1/T) at low temperatures (T ≤ 385 K, Fig. 6).

At the maximum oxygen concentration (value of γ=0.15) in the low-temperature range lnσ(1/T) curve (Fig. 6) of the SIPOS film, a region with a lower activation energy is clearly detected. However, according to the data from literature [4,5,8,17], in order to objectively estimate the activation energy in this region, it is necessary to cool the samples down to ~150 K. In addition, the magnitude of the activation energy of conductivity in this region depends on the oxygen content in the film and is due to the formation of an impurity subband [5]. In the high-temperature range (at T≥385 K) for the dependence lnσ(1/T) of SIPOS film (γ=0.15) the slope and the activation energy value increase to 0.63 eV (Fig. 6). The increase in the activation energy can be explained by the formation of a $SiO_{0/47}$ suboxide phase in the form of $SiOSi_3$ clusters with a band gap exceeding the corresponding silicon value. A similar increase in the activation energy of conductivity in the temperature range (T>300 K) with that in the oxygen content in the film was observed in the works [8,17].

4. Conclusions

The complex investigations by means of three independent methods XRD, Ultrasoft X-ray Emission Spectroscopy and Raman spectroscopy are shown, that the SIPOS layers obtained by means of LP CVD method at temperature 625 °C and SiH_4 silane rate 8 l/h with the addition of N_2O as an oxygen source at different values of $\gamma=N_2O/SiH_4=0\div0.15$ have a compound phase composition consisting of silicon nanocrystals, embedded in the amorphous matrix of silicon and silicon-oxygen clusters.

An increase in the oxygen content in the SIPOS layers to a maximum value at γ=0.15 leads to a decrease of nanocrystals size from ~75 nm (at γ=0) to 2–5 nm (at γ=0.15) immersed in an amorphous silicon matrix.

Oxygen in the amorphous silicon matrix is present in the bound form of silicon-oxygen $SiOSi_3$ type clusters corresponding to the known phase of the $SiO_{0.47}$ suboxide without the formation of SiO_2 dioxide.

These nonlinear qualitative and quantitative changes in the atomic and electron structure of the SIPOS layers caused by the bound oxygen result in a higher resistivity of the films by two orders of magnitude and increase the activation energy of conductivity as compared to silicon at temperatures above room temperature.

Credit author statement

1. Vladimir A. Terekhov: Conceptualization, Methodology, Validation, Writing - Original Draft, Supervision.
2. Dmitriy N. Nesterov: Funding acquisition, Investigation.
3. Konstantin A. Barkov: Formal analysis, Investigation, Visualization.
4. Evelina P. Domashevskaya: Writing - Review & Editing, Project administration.
5. Aleksandr V. Konovalov: Resources.
6. Yuriy L. Fomenko: Resources.
7. Pavel V. Seredin: Investigation, Validation.
8. Dmitriy L. Goloshchapov: Investigation, Formal analysis.
9. Anatoliy I. Popov: Resources, Methodology, Validation.
10. Aleksey D. Barinov: Investigation, Formal analysis.
11. Vyacheslav M. Andreeshchev: Investigation, Formal analysis.
12. Igor E. Zanin: Investigation.
13. Sergey A. Ivkov: Investigation, Formal analysis.
14. Oksana E. Loktionova: Investigation, Visualization.

Declaration of competing interest

The authors declare that they have no known competing financial interests or personal relationships that could have appeared to influence the work reported in this paper.

Acknowledgments

The reported study was funded by RFBR and Government of Voronezh region according to the research project № 19-42-363013.

The part of work was carried out with the support of the Ministry of Science and Higher Education of Russia Federation under the grand No. FZGU-2020-0036.In part of diagnostics of the structures the work of P.V. Seredin was supported by the RF President's Grants Council (Grant MD-42.2019.2).

References

[1] A. Mimura, H. Oohayashi, S. Murakami, N. Momma, High-voltage planar structure using SiO_2-SIPOS-SiO_2Film, IEEE Electron. Device Lett. 6 (1985) 189–191, https://doi.org/10.1109/EDL.1985.26092.

[2] A. Blicher, Field-Effect and Bipolar Power Transistor Physics, Academic Press, 1981. https://www.elsevier.com/books/field-effect-and-bipolar-power-transistor-physics/blicher/978-0-12-105850-0.

[3] A.S. Turtsevich, Obtaining semi-insulating silicon for high-voltage devices, Technology and design in electronic equipment, Technol. Des. Electron. Equip. 35 (2008) 35–41 [in Russian], http://dspace.nbuv.gov.ua/handle/123456789/52391.

[4] M. Hamasaki, T. Adachi, S. Wakayama, M. Kikuchi, Crystallographic study of semi-insulating polycrystalline silicon (SIPOS) doped with oxygen atoms, J. Appl. Phys. 49 (1978) 3987–3992, https://doi.org/10.1063/1.325356.

[5] M.L. Tarng, Carrier transport in oxygen-rich polycrystalline-silicon films, J. Appl. Phys. 49 (1978) 4069–4076, https://doi.org/10.1063/1.325367.

[6] J. Ni, E. Arnold, Electrical conductivity of semi-insulating polycrystalline silicon and its dependence upon oxygen content, Appl. Phys. Lett. 39 (1981) 554–556, https://doi.org/10.1063/1.92791.

[7] D. Dragomirescu, G. Charitat, Improving the dynamic avalanche breakdown of high voltage planar devices using semi-resistive field plates, Microelectron. J. 32 (2001) 473–479, https://doi.org/10.1016/S0026-2692(01)00017-9.

[8] M.J.B. Bolt, J.G. Simmons, The conduction properties of SIPOS, Solid State Electron. 30 (1987) 533–542, https://doi.org/10.1016/0038-1101(87)90209-7.

[9] E.P. Domashevskaya, V.A. Terekhov, S.Y. Turishchev, A.S. Prijimov, A.N. Kharin, E.V. Parinova, N.A. Rumyantseva, D.S. Usoltseva, Y.L. Fomenko, S.V. Belenko, Atomic and electronic structure of amorphous and nanocrystalline layers of semi-insulating silicon produced by chemical-vapor deposition at low pressures, J. Surf. Investig. 9 (2015) 1228–1236, https://doi.org/10.1134/S1027451015060257.

[10] JCPDS-international Centre for Diffraction Data ICDD PDF-2, Card № 01-077-2110.

[11] D. Joannopoulos, G. Lucovsky, The Physics of Hydrogenated Amorphous Silicon I, Springer-Verlag Berlin Heidelberg, 1984, https://doi.org/10.1007/3-540-12807-7.

[12] G. Wiech, H.O. Feldhütter, A. Šimůnek, Electronic structure of amorphous SiOx:H alloy films studied by x-ray emission spectroscopy: Si K, Si L, and O K emission bands, Phys. Rev. B 47 (1993) 6981–6989, https://doi.org/10.1103/PhysRevB.47.6981.

[13] S. Schamm, R. Berjoan, P. Barathieu, Study of the chemical and structural organization of SIPOS films at the nanometer scale by TEM-EELS and XPS, Mater. Sci. Eng. B Solid-State Mater. Adv. Technol. 107 (2004) 58–65, https://doi.org/10.1016/j.mseb.2003.10.010.

[14] Z. Iqbal, S. Vepřek, A.P. Webb, P. Capezzuto, Raman scattering from small particle size polycrystalline silicon, Solid State Commun. 37 (1981) 993–996, https://doi.org/10.1016/0038-1098(81)91202-3.

[15] I.H. Campbell, P.M. Fauchet, The effects of microcrystal size and shape on the one phonon Raman spectra of crystalline semiconductors, Solid State Commun. 58 (1986) 739–741, https://doi.org/10.1016/0038-1098(86)90513-2.

[16] Z. Li, W. Li, Y. Jiang, H. Cai, Y. Gong, J. He, Raman characterization of the structural evolution in amorphous and partially nanocrystalline hydrogenated silicon thin films prepared by PECVD, J. Raman Spectrosc. 42 (2011) 415–421, https://doi.org/10.1002/jrs.2711.

[17] M. Hamasaki, T. Adachi, S. Wakayama, M. Kikuchi, Electronic properties of Semi-Insulating Polycrystalline-Silicon (SIPOS) doped with oxygen atoms, Solid State Commun. 21 (1977) 591–593, https://doi.org/10.1016/0038-1098(77)90040-0.